

Towards Quantum Graph Neural Networks: An Ego-Graph Learning Approach

Xing Ai, Luzhe Sun, Junchi Yan, *Senior Member, IEEE*, Zhihong Zhang*,
and Edwin R Hancock, *Fellow, IEEE*

Abstract—Quantum machine learning is a fast-emerging field that aims to tackle machine learning using quantum algorithms and quantum computing. Due to the lack of physical qubits and an effective means to map real-world data from Euclidean space to Hilbert space, most of these methods focus on quantum analogies or process simulations rather than devising concrete architectures based on qubits. In this paper, we propose a novel hybrid quantum-classical algorithm for graph-structured data, which we refer to as the Ego-graph based Quantum Graph Neural Network (egoQGNN). egoQGNN implements the GNN theoretical framework using the tensor product and unity matrix representation, which greatly reduces the number of model parameters required. When controlled by a classical computer, egoQGNN can accommodate arbitrarily sized graphs by processing ego-graphs from the input graph using a modestly-sized quantum device. The architecture is based on a novel mapping from real-world data to Hilbert space. This mapping maintains the distance relations present in the data and reduces information loss. Experimental results show that the proposed method outperforms competitive state-of-the-art models with only 1.68% parameters compared to those models.

Index Terms—Quantum Computing, Quantum Machine Learning, Graph Neural Networks

1 INTRODUCTION

QUANTUM machine learning encapsulates a diverse variety of algorithms ranging from classical shallow learning techniques such as the Quantum Support Vector Machine (QSVM) [1], [2] and the quantum decision tree classifier [3] to the more recent quantum neural networks e.g. the Quantum Convolutional Neural Network (QCNN) [4], the Quantum Generative Adversarial Network (QGAN) [5] and the Quantum Graph Neural Network [6].

Distinct from the data processed by existing machine learning and deep learning techniques, the data used in quantum machine learning reside in high-dimensional Hilbert spaces represented in the form of quantum states. Maria et al. [7] point out that quantum machine learning algorithms overcome the problems associated with working in reduced dimensional space by using classical machine learning. Computation in high-dimensional Hilbert space can bring performance improvement. Seeking quantum counterparts of the Support Vector Machine (SVM) [8], Havlicek et al. [1] propose a quantum binary classification algorithm similar to SVM (QSVM). A quantum circuit is designed to map data from Euclidean space to Hilbert

space. However, the input dimension cannot exceed three. Schuld et al. [2] propose a quantum-classical kernel method. A quantum computer estimates the inner products of the data, while a classical computer calculates the estimation result and trains the algorithm. The Quantum Convolutional Neural Network (QCNN) [9] simulates the structure of the Convolutional Neural Network. For input sizes of N qubits, the QCNN has only $O(\log N)$ variational parameters. The Quantum Generative Adversarial Network (QGAN) of Hu et al. [5] has the potential for exponential acceleration relative to its classical counterpart. Hu et al. [5] demonstrate that after multiple rounds of training, the generator of QGAN can generate the corresponding quantum states with 98.9% fidelity. The generator is suitable for use on a medium-sized quantum computer in a noisy environment.

Recent work has aimed to combine quantum machine learning with graph representations [6], [10], [11], [12], [13]. Early work [6], [10], [11] constructed quantum circuit based models and showed these could successfully handle graph data. However, the input to these methods is the entire graph. The size of existing quantum devices is insufficient to handle this situation. The above models can thus only be applied to small-scale or synthetic datasets. More recently, motivated by the Graph Neural Tangent Kernel (GNTK) [14], Tang and Yan propose a novel quantum kernel for graph classification, referred to as the Graph Quantum Neural Tangent Kernel (GraphQNTK). This is equivalent to an infinite-width GNN with attention.

However, the above mentioned methods still suffer from two main limitations, namely (i) they lack a theoretical proof for being able to achieve graph isomorphism classification which we believe is a fundamental capability for expressive graph representation learning (in fact, we verify the discriminative ability of our model in our experiments) and (ii) there is no existing method for quantum graph learning

- Xing Ai is with School of Informatics, Xiamen University, Xiamen, Fujian, China. E-mail: 24320191152507@stu.xmu.edu.cn.
- Luzhe Sun is with Computer Science Department in University of Chicago, Chicago, IL, US. E-mail: luzhesun@uchicago.edu.
- J. Yan is with Department of Computer Science and Engineering, and MOE Key Lab of Artificial Intelligence, Shanghai Jiao Tong University, Shanghai 200240, China. E-mail: yanjunchi@sjtu.edu.cn.
- Corresponding author: Zhihong Zhang is with School of Informatics, Xiamen University, Xiamen, Fujian, China. E-mail: zhihong@xmu.edu.cn.
- Edwin R. Hancock is with University of York, York, UK. E-mail: edwin.hancock@york.ac.uk.

that maps Euclidean data into a quantum Hilbert space (and which we aim to address in our paper).

Graph-structured data or graph data are non-Euclidean and consist of nodes and edges. It is widely used in knowledge representation [15], social system analysis [16], [17], modelling higher-order interactions in physical systems [18], [19], and combinatorial optimization [20]. Recently, deep learning has achieved impressive results on a variety of tasks involving Euclidean data, and some studies have commenced generalizing deep learning to the graph domain.

Graph Neural Networks (GNNs) [21], are recently proposed neural network structures for the processing of graph-structured data. The main idea underpinning GNNs is the neighborhood aggregation strategy. The strategy updates the representation of a node by recursively aggregating the representations of its neighbors. Xu et al. [22] prove that a GNN which satisfies certain conditions is as powerful as the Weisfeiler-Lehman (WL) test [23] and can effectively distinguish the isomorphisms of graphs. Mathematically they prove GNNs can achieve the same effect as the WL test when three critical functions employed by the GNN are injective. Different realizations of the GNN include but are not limited to Relational Graph Convolutional Networks (R-GCN) [24], edge Graph Neural Networks (edGNN) [25], Random Walk Graph Neural Networks (RW-GNN) [26] and Factorizable Graph Convolutional Networks (Factor GCN) [27].

Recently, some studies have paid attention to introducing an ego-graph into the GNN to alleviate the limitations of GNNs [28] or to provide insights into their performance [29], [30]. An ego-graph consists of a central node and all of its connected neighbors. To address the scalability issue while applying an attention mechanism in GNNs, Zhao et al. [29] adopt a transformer model for ego-graphs rather than for the entire graph. Moreover, Zhu et al. [30] use ego-Graph information maximization to both analyze and provide theoretical guarantees on GNN transferability.

Motivated by the above methods, this paper proposes a hybrid classical-quantum machine learning approach to Graph Neural Network embodiment. Compared to the existing quantum algorithm for graph-structured data, our method is scale-free and able to utilize the features of nodes. Additionally, we ground the GNN framework in the physical elements of quantum computing, i.e. qubits.

Our main contributions are summarized as follows:

- 1) A novel quantum-classical hybrid machine learning algorithm for graph-structured data is proposed, namely the Ego-graph based Quantum Graph Neural Network (egoQGNN). It utilizes the tensor product and unitary matrix representations to implement the theoretical framework of the GNN. Due to the fact that the unitary matrix only requires the specification of a rotation angle, i.e. the variational parameter, the egoQGNN achieves a similar performance but with only 1.68% of the parameters when compared with the GNN model with the least parameters, DGCNN [31].
- 2) We design an ego-graph decomposition processing strategy to decompose a large graph into small ego-

graphs which can be handled by existing small-sized quantum devices. By exploiting this strategy, the egoQGNN can handle larger-sized graph-structured data with a fixed-sized quantum device, via the efficient use of qubits. In the current situation where the number of physical qubits is limited, this is an important feature of our method.

- 3) A trainable method for mapping data from a Euclidean space to a quantum Hilbert space is proposed. This can both maintain distance relations and also reduces information loss during the mapping.

The remainder of this paper is organized as follows. Section II reviews the existing GNNs and quantum machine learning algorithms. Section III introduces the fundamental concepts of quantum machine learning and GNNs. Section IV introduces the trainable mapping method, the theoretical framework, and the resulting structure of the egoQGNN. Section V presents our experimental results obtained using the egoQGNN. Finally, Section VI concludes the paper and offers directions for future investigation.

2 RELATED WORK

In this section, we briefly review two related topics, namely 1) graph neural networks, especially those for graph level embedding; and 2) quantum machine learning.

2.1 Graph Neural Networks

The goal of graph neural networks is to map both node features and structural arrangement information to vectorized representations that can be used to embed graphs into lower-dimensional spaces or manifolds. GNNs leverage node features and edge features to learn the representation of each node within a graph. By embedding the nodes of a graph and combining all the node embeddings within a graph, GNNs obtain the required graph representation.

Since the seminal work in [32], a diverse set of GNN models have been proposed. For example, it has been proven [22] that a GNN that satisfies certain restrictive conditions can be as powerful as the Weisfeiler-Lehman (WL) test [23] and can effectively distinguish the isomorphisms of graphs. Mathematically it has been proved that GNNs can achieve the same effect as the WL test when three critical functions used by the GNN are injective. This analysis has been further extended to directed graphs by aggregating nodes and edges at the same time [25]. Spectrally-based GNNs [33], [34], [35] define spectral filter operations based on the Laplacian matrix of a graph. This is done by defining a series of filter coefficients based on the Laplacian eigenvalues and eigenvectors, and are thus computationally expensive. Fast and Deep Graph Neural Networks (FDGNN) [36] make it possible to combine the advantages of the deep architectural construction of GNNs with the extreme efficiency of randomized neural networks, and in particular RC, methodologies. Random Walk Graph Neural Network (RWGNN) [26] generates graph representations by comparing a set of trainable *hidden graphs* against input graphs using a variant of the P -step random walk kernel.

GNNs have achieved state-of-the-art results on different graph learning tasks, such as graph classification, link prediction and semi-supervised node classification. However, GNNs embed nodes into Euclidean space and cause significant distortion and structure. To overcome this problem, several GNN models based on non-Euclidean geometry have been proposed [37] [38] [39] [40]. These methods preserve the hierarchical structure of the graph and have improved performance compared to Euclidean GNNs. One common feature shared by these methods and our model is that of computing graph representation in a non-Euclidean space.

2.2 Quantum machine learning

Recently, there has been increasing interest in generalizing quantum computation to the machine learning domain. Several studies [1], [2], [5], [8], [9] have been proven to be effective for classification. Unlike most classical machine learning methods, which process data in a Euclidean space, quantum machine learning methods map data to quantum states residing in a high dimensional complex-valued Hilbert space. Due to quantum entanglement, the dimensionality of the Hilbert space increases exponentially with the number of qubits. For example, the dimensionality of an n qubit Hilbert space is 2^n . This means that quantum states in this Hilbert space are 2^n dimensional complex vectors. In Section III, we will introduce the fundamentals of quantum machine learning in more detail. Some observations that can be drawn from these methods are (i) the inputs of these methods are quantum states defined in terms of qubits; (ii) the methods utilize quantum gates with learnable parameters to train the model and a classical computer is responsible for training, measuring and controlling quantum devices; (iii) the methods classify data by measuring the quantum state rather than applying softmax or similar functions. More details given in Section IV.

For graph structured data, some studies have attempted to utilize quantum machine learning to capture structural information and obtain graph or node representations in a quantum Hilbert space. Verdon et al. [6] were the first to propose a quantum computing based graph classification model, the so-called Quantum Graph Neural Network (QGNN). This captures graph structure using a quadratic Hamiltonian and utilizing quantum circuits to extract relevant graph structural information. With the aim of overcoming the 1-WL limitation of existing GNNs, Péter et al. introduce the Equivalent Quantum Graph Circuit (EQGC) [11]. This captures the permutation-invariant topologies of the input graphs. However, due to the number of required qubits scaling linearly with the number of nodes, EQGC can only handle small-scale synthetic datasets. The Graph Quantum Neural Tangent Kernel (GraphQNTK) is the only known quantum algorithm that can handle realistically sized graph data. Similar to the Graph Neural Tangent Kernel (GNTK) [14], GraphQNTK is essentially a graph kernel and is equivalent to an infinite-width GNN.

The above quantum models have been successfully applied to graph-related tasks. However, most accept only low-dimensional data or pure quantum states as input. Two important problems limit the application of these methods

to real-world large-scale data. Firstly, there is a lack of general methods to map data from a Euclidean space into a quantum Hilbert space. Secondly, due to the limited number of available qubits, real-world high-dimensional graph data can not be loaded into these quantum circuits. Besides, all of the above methods lack solid theoretical guarantees for the graph isomorphism classification problem. We also note that there are also related quantum computing studies on both node classification [12], [41], [42] and link prediction [43]. None of this work is grounded in a theoretical analysis or proof of graph isomorphism.

In this paper, we propose a novel hybrid quantum-classical machine learning method referred to as the Ego-graph based Quantum Graph Neural Network (egoQGNN), which is a quantum computing based model for graph classification. By introducing the ego-network compositional processing strategy (Sec. 4.4), the egoQGNN can be applied to real-world data and is not limited by the number of available qubits. The egoQGNN also implements the theoretical framework of GNNs using operations available in a quantum computer and utilizes a unitary weight matrix together with a Hilbert-space tensor product. As a result, the egoQGNN empowers a quantum computer with the ability to classify graphs.

As shown in Table 1, as a hybrid quantum-classical algorithm, our model uses a hierarchical architecture to capture information within k -hop neighbors of a node. Moreover, the proposed model is able to apply to graph isomorphism tests since it provides a theoretical analysis and proof of this capability in Sec. 4.1. With the proposed decomposition strategy, our model can handle real-world datasets.

3 PRELIMINARIES

In this section, we briefly review the underlying concepts which will be exploited in the development of a novel quantum neural network reported in this paper. Firstly, we introduce the fundamental concepts of quantum machine learning. Secondly, we review the fundamental theory of the GNN. In order to make our description clearer, we list the notation used in this paper in Table 2.

3.1 Fundamentals of Quantum Machine Learning

In order to introduce our new quantum neural network more clearly, we will introduce some of the fundamental elements of quantum machine learning including the quantum bit, quantum gate and quantum circuit.

Quantum bit: Quantum bits or qubits for short, are analogous to the classical binary bit which are the fundamental elements of classical computation. The qubit is a mathematical construct with certain specific formal properties. Unlike the classical bit with binary states 0 or 1, the quantum state of a qubit is a 2-dimensional complex-valued vector formed by linear combinations of the basis vectors $|0\rangle$ and $|1\rangle$:

$$|0\rangle = (0, 1)^T \quad |1\rangle = (1, 0)^T \quad (1)$$

Suppose the quantum state of a qubit is $|\varphi\rangle$:

$$|\varphi\rangle = \alpha|0\rangle + \beta|1\rangle = (\alpha, \beta)^T \quad (2)$$

TABLE 1

Comparison of the existing quantum graph representation learning methods, shows each model: is a hybrid quantum-classical algorithm or not, is able to apply to graph isomorphism or not, has hierarchy architecture or not, can handle real-world datasets or not

Models	Hybrid	Graph Isomorphism	Hierarchy architecture	Real-World dataset
QCNN [6]	No	No	Yes	No
QGCN [10]	No	No	Yes	No
EQGC [11]	Yes	No	No	No
QGCNN [44]	Yes	No	No	No
GraphQNTK [13]	Yes	No	No	Yes
egoQCNN(ours)	Yes	Yes	Yes	Yes

TABLE 2
Notations and their descriptions

Symbol	Definition
h_v^t	node v 's representation of t -th iteration
$\mathcal{N}(v)$	a set of nodes adjacent to node v .
σ	activation function
W^t	weight matrix of t -th iteration
$ \varphi\rangle, \langle\varphi $	Quantum state and its complex conjugate transpose
U, U^\dagger	arbitrary unitary matrix and corresponding adjoint
H	Hadamard gate
X, Y, Z	X gate, Y gate, Z gate
RX, RY, RZ	rotation operators about the Pauli-X, Pauli-Y, Pauli-Z axes
\otimes	tensor product

The numbers α and β are complex numbers that satisfy the condition:

$$|\alpha|^2 + |\beta|^2 = 1 \quad (3)$$

Due to the above condition in Eq(3), the quantum state of a qubit is a point on the unit 3-dimensional sphere, referred to as the Bloch sphere. The Bloch sphere resides in a Hilbert space, and there are three basis vectors in this space, namely Pauli-X, Pauli-Y, and Pauli-Z. Any quantum state on the Bloch sphere makes angles with the three bases, as shown in Fig. 3.

There are an infinite number of points on the Bloch sphere. In other words, a qubit can represent an infinite number of quantum states, while a classical bit can only represent two states, i.e. 0 or 1. So, a qubit has a greater representational capacity than a classical bit. If a physical system, e.g. a quantum computer, has more than one qubit, for instance, n qubits, then the quantum state of this physical system is the tensor product of all its constituent qubits or quantum states:

$$|\phi\rangle = |\varphi_1\rangle \otimes |\varphi_2\rangle \otimes \cdots \otimes |\varphi_n\rangle \quad (4)$$

The tensor product of n qubits is a 2^n -dimensional complex vector. So, the dimensionality of the quantum state of a system increases exponentially with the number of qubits that constitute it.

Quantum gate: A classical computer has logic gates that change the states of bits, and these include the AND gate, OR gate, and NOT gate. For quantum computers, quantum gates are used to change the quantum states of the qubits. After the quantum gate acts on the quantum state represented by a qubit, this quantum state is transformed, i.e. rotated, to give another vector. Quantum gates can be divided into single qubit gates and multiple qubit gates.

Single qubit gates are applied to a single qubit state. Multiple qubit gates are applied to several qubit systems to transform their quantum states. Multiple qubit states can be obtained from the multiplication or tensor product of a single qubit gate. The transformation of states performed by the gate can be represented using a unitary matrix since the results of both a tensor product or a multiplication of quantum gates is a unitary transformation.

Quantum circuits: A classical computer can be represented in terms of circuits containing connections and logic gates. Similarly, a quantum computer can be represented using quantum circuits containing connections and quantum gates. For a quantum computer, each connection represents a qubit, which is used to carry information, and the quantum gates perform manipulations to transform the quantum state.

3.2 Graph Neural Networks on Graph Classification

Graph Neural Networks (GNNs) are effective machine learning tools for structured data and rely on a neighborhood aggregation strategy. Specifically, for each node in a graph, the GNN recursively aggregates the current representation with those for its neighbors, thus giving a new representation for use at the next iteration. For graph classification, Xu et al. [22] demonstrate that three crucial functions of GNNs, namely AGGREGATE, COMBINE and READOUT, must each be injective multi-set functions, for example, a sum. Formally, the k -th interaction of a GNN can be expressed as:

$$\begin{cases} h_{\mathcal{N}(v)}^k = AGG^{(k)}(\{h_\mu^{(k-1)}, \forall \mu \in \mathcal{N}(v)\}) \\ h_v^k = \sigma(W^k \cdot COM^{(k)}(h_v^{(k-1)}, h_{\mathcal{N}(v)}^k)) \end{cases} \quad (5)$$

where h_v^k is the feature vector of node v at the k -th iteration, and $\mathcal{N}(v)$ is the set of nodes adjacent to v .

Here, the READOUT function aggregates the representations of all nodes from the final iteration to obtain the complete graph representation h_G :

$$h_G = READOUT(\{h_v^K | v \in G\}) \quad (6)$$

The GNN model presented by Xu et al. [22] can be represented as follows:

$$h_v^k = \sigma(h_v^{(k-1)} W_1^{(k-1)} + \sum_{\mu \in \mathcal{N}(v)} h_\mu^{(k-1)} W_2^{(k-1)}) \quad (7)$$

where $W_1^{(k-1)}$ and $W_2^{(k-1)}$ are trainable weight matrices at the k -th iteration for node v and its neighbors respectively.

4 METHODOLOGY

In this paper, we develop a novel quantum-classical hybrid machine learning algorithm for graph-structured data. The idea is to develop a quantum GNN by designing a quantum circuit and replacing the Euclidean weight matrices of the GNN with unitary matrices, i.e. quantum gates. In this way, we incorporate theoretical ideas from quantum machine learning into deep learning in the graph domain.

In this section, we first introduce the theoretical framework underpinning our model and provide mathematical proof. Then, we introduce the quantum circuit to implement the egoQGNN, the trainable mapping method and the sequential compositional processing strategy. Finally, we introduce the structure and explain how the egoQGNN can be used to classify quantum states. We then summarize the processes underpinning the egoQGNN.

4.1 Theoretical Framework of egoQGNN

To distinguish graph isomorphisms by quantum machine learning, we follow the study of Xu et al. [22], and introduce the theoretical framework for GNNs using quantum machine learning. What makes the GNN so powerful is its injective aggregation strategy, which maps different nodes to different representational units. As a result, different graphs have different representations.

The GNN model [22] can be represented by:

$$\mathbf{h}_v^k = \sigma \left(\mathbf{h}_v^{(k-1)} \mathbf{W}_1^{(k-1)} + \sum_{\mu \in \mathcal{N}(v)} \mathbf{h}_\mu^{(k-1)} \mathbf{W}_2^{(k-1)} \right) \quad (8)$$

where \mathbf{h}_v^t is the representation of node v at the t -th iteration and $\mathcal{N}(v)$ is the neighbor set of node v . The matrices $\mathbf{W}_1^{(k-1)}$ and $\mathbf{W}_2^{(k-1)}$ are respectively trainable weight matrices at the $(k-1)$ -th layer for node v and its neighbors; σ is the network activation function.

The aim of this paper is to provide a route to implementing Eq. 8 on a quantum computer. For quantum computing, the state of a physical system composed of several qubits is obtained by a tensor product of the individual qubit quantum states, namely quantum entanglement. The tensor product is one of the fundamental constructs of quantum computing. Due to its ability to enlarge the space exponentially, the tensor product can be used to map different nodes to different representations. The tensor product is analogous to the summation operation in classical GNNs. In other words, both the tensor product and the summation are injective functions.

Lemma 1. *The tensor product is injective, for non-zero vectors with the same dimension. As a result, the tensor product maps them to different representations unless they are linearly dependent vectors.*

All the proofs including that for this Lemma can be found in the Appendix. Since quantum states are complex vectors, according to Lemma 1, the tensor product maps different quantum states to different representations. Moreover, all quantum states are linearly independent.

Lemma 2. *If two quantum states \mathbf{A} and \mathbf{B} are linearly dependent, and $\mathbf{B} = k \cdot \mathbf{A}$, then $k = \pm 1$.*

Due to the property of quantum states, Lemma 2 can be demonstrated easily using the proof in the Appendix.

According to Lemma 1 and Lemma 2, the tensor product maps two quantum states to the same representation if and only if the two quantum states are identical.

So, for the egoQGNN, the tensor product replaces the summation of the GNN, and Eq. 8 becomes:

$$\mathbf{h}^{t-1}(v) \rightarrow |\varphi_v\rangle^{t-1}, \quad \mathbf{h}^{t-1}(\mu) \rightarrow |\varphi_\mu\rangle^{t-1} \quad (9)$$

$$|\varphi_v\rangle^t = \mathbf{U}_1 |\varphi_v\rangle^{t-1} \otimes \left(\bigotimes_{\mu \in \mathcal{N}(v)} \mathbf{U}_2 |\varphi_\mu\rangle^{t-1} \right) \quad (10)$$

$$\mathbf{h}^t(v) = -\text{tr}(\rho^t \log \rho^t), \quad \rho^t = |\varphi_v\rangle^t \langle \varphi_v|^t \quad (11)$$

where \mathbf{U}_1 and \mathbf{U}_2 are unitary matrices with trainable parameters, which correspond to the Euclidean weight matrices \mathbf{W}_1 and \mathbf{W}_2 in the GNN of Eq. 8. Unlike the weight matrices of the classical GNN which have many numerical parameters which must be trained, the unitary matrices have only a single variational parameter that represents the rotation angles of the quantum states. Details regarding unitary matrices and their properties are given in the Appendix.

Note that Eq. 10 implements on a quantum computer and returns the result to a classical computer. We will discuss the implementation of Eq. 10 in the next section. Eq. 9 is achieved by the proposed mapping method. The representation of the next layer can be obtained by von Neumann entropy in Eq. 11.

Both Eq. 8 and Eq. 10 are able to distinguish non-isomorphic graphs, i.e. perform graph classification. To demonstrate the effectiveness of the egoQGNN for the graph isomorphism problem, we need to prove that Eq. 10 will map nodes with different features or neighbors to different representations.

Lemma 3. *For different nodes v and μ , the outputs of Eq. 10: $|\varphi_v\rangle$ and $|\varphi_\mu\rangle$, meet $|\varphi_v\rangle \neq |\varphi_\mu\rangle$.*

A natural follow-up theorem is that the egoQGNN can distinguish graphs that are decided as non-isomorphic graphs by the GNNs based on Eq. 8.

Theorem 1. *The egoQGNN maps two non-isomorphic graphs G_1 and G_2 as decided via a GNN by Eq. 10 to different embeddings.*

Compared with the GNN, the main differences provided by the egoQGNN are the tensor product aggregation operator and the unitary matrix. The advantages of using the tensor product and unitary matrix are as follows:

1) The tensor product enlarges the node representation space exponentially. As a result, nodes with different features can be mapped to different representations. Although alternative functions such as the dot product and matrix multiplication are both injective functions, their implementations on quantum devices are not as convenient as the tensor product. This is because the tensor product is a fundamental facet of quantum computing.

2) Since the tensor product can enlarge the representation space exponentially, the egoQGNN has significantly fewer parameters than related deep learning models. A layer of the GNN requires a $d \times h$ weight matrix to transform a d -dimensional input into a h -dimensional output. Such a layer has $d \times h$ parameters that need to be trained. For the egoQGNN, the entanglement of $\max(\log_2 d, \log_2 h)$

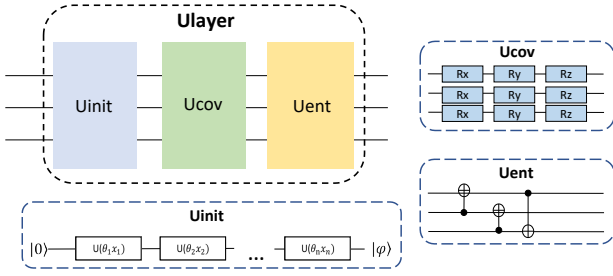


Fig. 1. Ulayer with Uunit, Ucov, and Uent. Uunit contains n quantum gates to map n -dimensional data X into quantum states. In Ucov, RX, RY, RZ quantum gates are applied to each qubit. Uent utilizes CNOT gates to entangle all qubits.

qubits can generate $\max(d, h)$ -dimensional quantum states. The egoQGNN has only $n \cdot \max(\log_2 d, \log_2 h)$ variational parameters for training if n quantum gates are applied to each qubit. This is because a unitary matrix has only one variational parameter (the rotation of the quantum states).

4.2 Quantum Circuit of egoQGNN

To implement Eq. 10 on a quantum device, we design a quantum circuit with a hierarchical structure similar to that of the GNN. The quantum circuit we have designed contains K Ulayers to capture the information within the K -hop neighbors of a node. A Ulayer includes three components: Uunit, Ucov and Uent. This is illustrated in Fig. 1. For n input nodes, the initial states of the quantum circuit are $|0\rangle^{\otimes n}$. The output is the tensor product of the quantum states over all the qubits.

We allocate a quantum circuit and the requisite qubits to the ego-graphs consisting of a node and its neighbors. After the required computations have been completed, we then free the quantum circuit and its qubits for future use.

The Uunit component maps the data to quantum states, which corresponds to the quantum circuit of the trainable mapping method (described later in this section). Specifically, it is responsible for mapping node features from Euclidean space to Hilbert space. The Ucov component, on the other hand, has three quantum gates on each qubit: RX, RY, RZ. Each quantum gate accepts one trainable parameter. All neighbors of a node share parameters but do not include the node. For an arbitrary qubit of the Ucov component, if the input quantum state is $|\varphi_{in}\rangle$, the output is $|\varphi_{out}\rangle$:

$$|\varphi_{out}\rangle = \mathbf{U}_{cov}|\varphi_{in}\rangle = \mathbf{RX}(\theta_x)\mathbf{RY}(\theta_y)\mathbf{RZ}(\theta_z)|\varphi_{in}\rangle \quad (12)$$

The \mathbf{U}_{cov} corresponds to \mathbf{U}_1 or \mathbf{U}_2 in Eq. 10. $\theta_x, \theta_y, \theta_z$ are variational parameters of quantum gates. The output of Ulayer is a tensor product over the quantum states of all nodes, corresponding to $|\varphi_v\rangle^t$ in Eq. 10. Therefore, the Ulayer component implements Eq. 10. In a manner similar to the GNN, the egoQGNN can aggregate features of the k -hop neighbors to a node by applying K Ulayers. Ucov is followed by a Uent component, which applies a CNOT gate to each pair of qubits to entangle their information. The parameters of the Uunit component have been trained and will not be updated during the training of Ulayer.

Considering the likely effects of noise interference on quantum devices, we apply the three-bit error correction

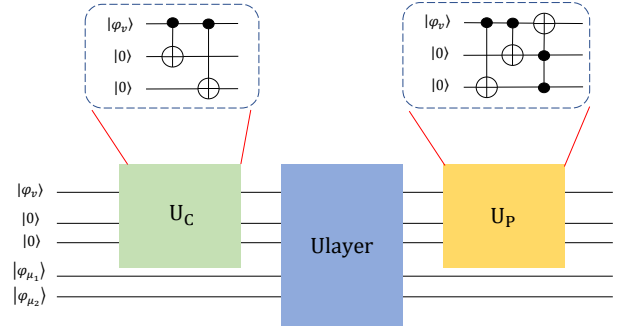


Fig. 2. Following the three-bit error correction code proposed by [45], the error correction of egoQGNN can be achieved by applying U_C and U_P modules after and before Ulayer respectively.

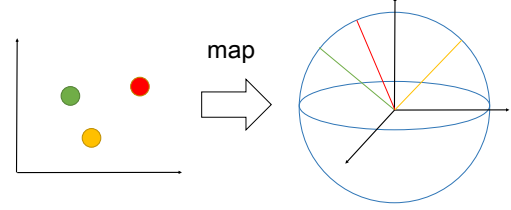


Fig. 3. In Euclidean space, the distance between the green point and the orange one is smaller than that between the green and the red ones. After mapping the data points to Hilbert space, points close to each other in Euclidean space become more distant quantum states (the green and orange lines), while the distance between the points which are farther away in Euclidean space becomes closer (the red and green lines).

code [45] to the above circuit. According to Eq.(10), the goal of the egoQGNN circuit is to aggregate the neighboring quantum states ($|\varphi_\mu\rangle$) into the quantum state of the node v ($|\varphi_v\rangle$) to update the representation of the node v . To avoid the interference of noise on the representation of the node v , the components U_C and U_P are respectively applied before and after the application of the Ulayer. Specifically, U_C first copies the information from the target bit to the two auxiliary qubits via two CNOT gates. After applying the Ulayer, U_P applies three CNOT gates to assist the recovery of the state of the target qubit $|\varphi_v\rangle$, as shown in Fig. 2.

4.3 Trainable Mapping Method

Existing quantum machine learning techniques [1], [4], [5], [46], [47], [48] are mainly applied to artificial data or small-scale real-world data. One reason for this restriction is the lack of an effective mapping from a variety of real-world data types to quantum states. To address this problem, we propose trainable mapping to maintain the distances between data and to reduce information loss resulting from the mapping.

Quantum states are distributed on the surface of the Bloch sphere that resides in Hilbert space. Mapping data from a Euclidean space to the Bloch sphere may incur a large distortion, as shown in Fig. 3.

The distance relations between the quantum states on the Bloch sphere are expected to be consistent with those between the data in Euclidean space. Any two sample points that are close to each other in Euclidean space should also be close after the mapping to Hilbert space. If this is not the case, the distance difference between the quantum states and the data will induce information loss and impair the subsequent analysis operations. Considering the

above problem, we present a mapping method in which the loss is related to the difference in the distance relations between the Euclidean space and the Bloch sphere. The corresponding circuit implementation for this method is shown in the Uinit component of Fig. 1. For n -dimensional data $\mathbf{x} = (x_1, x_2, \dots, x_n)$, the mapping circuit repeatedly uses a qubit with n quantum gates to map each sample to a corresponding quantum state. Each quantum gate accepts the product of the x_i and the trainable parameter is θ_i . Obviously, the Euclidean distance is not suitable for distance measurement on the Bloch sphere, which is a unit sphere. We utilize the inverse cosine of the inner product of the quantum states for distance measure. The reason that we chose inverse cosine is the low computational complexity and natural consistency with the spherical representation. We believe other non-Euclidean distance measures are also available for our model, e.g. hyperbolic distances.

We construct a loss based on the correlation matrix \mathbf{D} and \mathbf{D}' of the data and the corresponding quantum states:

$$\mathbf{D}'_{ij} = \frac{\arccos(\langle \varphi_i | \varphi_j \rangle)}{\max(\mathbf{D}')}, \quad L_{map} = \sum_{i=1}^n \sum_{j=1}^n |\mathbf{D}_{ij} - \mathbf{D}'_{ij}| \quad (13)$$

where \mathbf{D}_{ij} is the normalized Euclidean distance between samples i and j . Similarly \mathbf{D}'_{ij} is the normalized distance defined in Eq. 13 between quantum state i and j .

Compared with the existing mapping methods for quantum algorithms, the main difference of the proposed mapping method is applying trainable parameters to maintain the distance relationships between data and quantum states, and which reduces information loss. Our experiments will show the effectiveness of this approach.

4.4 Ego-graph Decompositional Processing Strategy

One bottleneck for quantum machine learning is the lack of available physical qubits in handling real-world data.

For efficient use of the available qubits, we propose a decompositional processing strategy based on an ego-graph decomposition. Concretely, according to Eq. 8 and Eq. 10, the iterative updating of the representation of node v is obtained by aggregating node v together with its neighbors $N(v)$ at the current iteration. As a result, the iterative updating of each node in a graph is only related to its neighbors. Therefore, we regard a node and its neighbors as an ego-graph. A graph containing N nodes can be decomposed into N ego-graph. The egoQGNN computes the representation of each ego-graph sequentially. As such, the process only requires a fixed number of qubits.

To commence, the entire graph is divided into ego-graph using a classical computer. The number of ego-graph is equal to the number of nodes. Next, the quantum circuits process each ego-graph sequentially and return their representations to the classical computer. Finally, the ego-graph representations are re-merged to reconstitute the original graph representation using the classical computer.

For a graph with N nodes, the number of qubits required to compute its representation is accordingly reduced from N to D by introducing the above ego-graph decomposition, where D is the maximum degree of the graph. If the number of available qubits $n < D$, we can divide the neighbour sets

Algorithm 1 Decompositional processing for a graph

Input: $G = (V, E)$, $|V| = N$; node features $X = \{x_v | \forall v \in V\}$.
Output: ego-graph set $\{S_v | \forall v \in V\}$, ego-graph features set $\{C_v | \forall v \in V\}$.

```

1: for  $v \in V$  do
2:   add  $v$  and  $N(v)$  to  $S_v$ ;
3:   for  $\mu \in N(v)$  do
4:     add  $X_\mu$  to  $C_v$ ;
5:   end for
6: end for

```

Algorithm 2 Trainable mapping for quantum representation

Input: input features $X = \{x_v \in \mathbb{R}^d | \forall v \in V\}$, random initial parameters of mapping circuit $P \in \mathbb{R}^d$, the mapping circuit MC .
Output: trained initial parameters of mapping circuit $P_t \in \mathbb{R}^d$.

```

1: for  $i \in V$  do
2:   for  $j \in V$  do
3:      $\mathbf{D}_{ij} = x_i \cdot x_j$ ;
4:   end for
5: end for
6: for  $i \in V$  do
7:    $|\varphi_i\rangle \leftarrow MC(P, x_i)$ ;
8: end for
9: for  $i \in V$  do
10:  for  $j \in V$  do
11:     $\mathbf{D}'_{ij} = \arccos(\langle \varphi_i | \varphi_j \rangle)$ ;
12:     $L_{map} = L_{map} + |\mathbf{D}_{ij} - \mathbf{D}'_{ij}|$ ;
13:  end for
14: end for
15:  $P_t = \operatorname{argmin}_P Loss$ ;

```

$\mathcal{N}(v)$ of node v into M sets: $\mathcal{N}(v) = \mathcal{N}_1(v) \cup \mathcal{N}_2(v) \cup \dots \cup \mathcal{N}_m(v)$. All sets satisfy the conditions:

$$|\mathcal{N}_i(v)| \leq n, \quad \mathcal{N}_i(v) \cap \mathcal{N}_j(v) = \emptyset, \quad i, j \in [1, m], i \neq j \quad (14)$$

We sequentially compute the representations of the sets as follows:

$$|\varphi_{v_i}\rangle^{t-1} = \bigotimes_{\mu \in \mathcal{N}_i(v)} \mathbf{U}_2 |\varphi_\mu\rangle^{t-1} \quad (15)$$

$$|\varphi_v\rangle^t = \mathbf{U}_1 |\varphi_v\rangle^{t-1} \bigotimes \left(\bigotimes_{i \in [1, m]} |\varphi_{v_i}\rangle^{t-1} \right), \quad i \in [1, m] \quad (16)$$

Eq. 16 is computed using the classical computer, as $|\varphi_{v_i}\rangle^{t-1}$ is stored in the classical computer.

For the effectiveness of the decompositional processing strategy, we provide the following results.

Theorem 2. For the same inputs, Eq. 16 is equivalent to Eq. 10.

We provide proof of this theorem in the Appendix.

4.5 Structure of the egoQGNN

The output of the quantum circuit is a tensor product over the quantum states of all the nodes, giving a high-dimensional vector. To classify graphs, their von Neumann entropy is summed over the quantum states of all nodes and used as a characterization of the graph.

The classical Shannon entropy measures the uncertainty associated with a classical probability distribution for a set of data. Quantum states can be described in a similar way

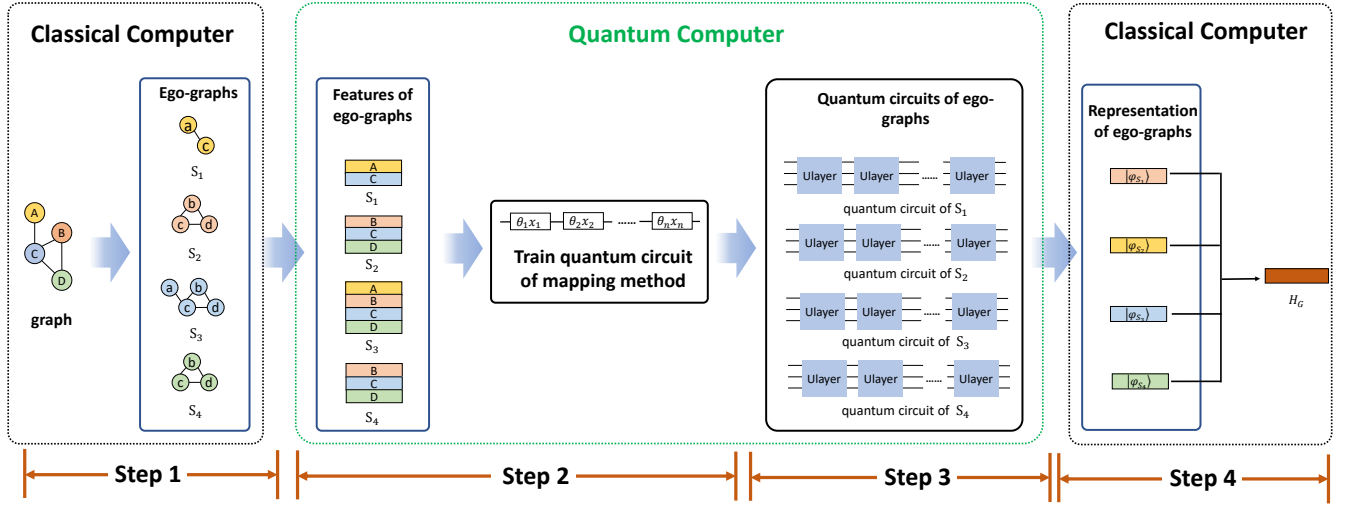


Fig. 4. An instance of the egoQGN. Step 1 and Step 4 are implemented on a classical computer. The quantum circuits of Step 2 and Step 3 can run on a quantum circuit or simulator of a classical computer.

using density operators in place of probability distributions, and the von Neumann entropy in place of the Shannon entropy. For a system with pure quantum state $|\varphi_i\rangle$ the density matrix is $\rho = \sum_i |\varphi_i\rangle\langle\varphi_i|$, and the graph representation \mathbf{h}_G is:

$$\mathbf{h}_G = \sum_{v \in G} S(\rho_v), \quad \rho_v = |\varphi_v\rangle\langle\varphi_v| \quad (17)$$

$$S(\rho_v) = -\text{tr}(\rho_v \log \rho_v) \quad (18)$$

For the binary classification problem, the Quantum Support Vector Machine (QSVM) [1] classifies data by measuring components of quantum states along the Pauli-Z direction. The quantum states on the upper Bloch hemisphere are assigned to one class and the quantum states on the lower Bloch hemisphere are assigned to the other class. Our approach is essentially the same as QSVM. We use two quantum states corresponding to two classes, and these correspond to the upper and lower Bloch hemispheres. The von Neumann entropies of two quantum states are ρ_0 and ρ_1 . Suppose \mathbf{h}_G is the representation of graph G to be classified, the label y_G of graph G is:

$$y_G = \begin{cases} 0, & \text{if } |\rho_0 - \mathbf{h}_G| \geq |\rho_1 - \mathbf{h}_G| \\ 1, & \text{else} \end{cases} \quad (19)$$

More details about the training of the egoQGN are given in the Appendix. The egoQGN consists of the following processing steps, where K is the number of iterations.

Step 1) Classical computer decomposes graph into ego-networks.

Step 2) Train the circuit of the mapping method with node features. The trained parameters of the circuit are stored on a classical computer. After training, the node features of the ego-networks are mapped into quantum states by applying the circuit.

Step 3) The quantum device runs the quantum circuit to compute the representations of the different ego-networks sequentially. The classical computer stores all the representations computed in this way.

Step 4) A classical computer computes the entropies of the individual representations and combines them using Eq. 18.

Algorithm 3 Framework of our egoQGN

Input: Ego-graph set $\{S_v | \forall v \in V\}$ with features $\{C_v | \forall v \in V\}$, the quantum circuit of egoQGN mentioned in Sec. 4.2 QC , Predefined von Neumann entropies of two classes: ρ_0 and ρ_1 .

Output: label prediction for graph G : l_G .

- 1: **for** $v \in V$ **do**
- 2: $|\varphi_v\rangle \leftarrow QC(S_v, C_v)$;
 $\rho_v = |\varphi_v\rangle\langle\varphi_v|$;
- 3: **end for**
- 4: $\mathbf{h}_G = \sum_{v \in V} \rho_v$;
- 5: $y_G = \begin{cases} 0, & \text{if } |\rho_0 - \mathbf{h}_G| \geq |\rho_1 - \mathbf{h}_G| \\ 1, & \text{else} \end{cases}$

Step 5) Steps 1-4 are repeated to obtain graph representations for classification. Fig. 4 shows the structure.

4.6 Summary of the egoQGN Framework

We summarize the framework of egoQGN, whose decompositional processing strategy is shown in Alg. 1. This corresponds to step 1 of Fig. 4, running on a classical computer. Alg. 2 involves step 2 of Fig. 4. After training, Alg. 2 outputs the initial parameters of the mapping circuit. Step 3 and step 4 of Fig. 4 are summarized in Alg. 3, whose output is the label assigned to the input graph.

5 EXPERIMENTS

In this section, we perform evaluations of the proposed egoQGN model on the graph classification task. We compare the egoQGN to both state-of-the-art graph kernels and deep learning methods. We conduct experiments on six standard graph classification benchmarks.

5.1 Datasets and Baselines

An overview summary of the datasets used in our experiments is given in Table 4. The data includes MUTAG [53], four variants of PTC [54] and PROTEINS [55]. For all of

TABLE 3
Statistics of the used graph datasets.

Datasets	MUTAG	PTC_MR	PTC_FM	PTC_MM	PTC_FR	PROTEINS
Max # nodes	28	109	64	64	64	620
Mean#nodes	17.9	14.1	14.1	14.0	14.5	39.1
Mean # edges	19.8	14.7	29.0	28.63	30.0	72.82
# graphs	188	344	349	336	351	1113
# node labels	6	18	18	20	19	61
# edge labels	3	4	4	4	4	-
# classes	2	2	2	2	2	2

TABLE 4
Evaluation for graph classification accuracy over six benchmarks (in % \pm standard error).

Datasets	MUTAG	PTC_FM	PTC_FR	PTC_MM	PTC_MR	PROTEINS
WL [49]	90.4 \pm 5.7	60.4	65.7	66.6	59.9 \pm 4.3	75.0 \pm 3.1
CSM [50]	85.4	63.8	65.5	63.3	58.1	-
DGCNN [31]	85.8	57.31 \pm 4.2	63.5 \pm 3.9	60.96 \pm 8.4	58.6	70.9 \pm 2.8
R-GCN [24]	81.5	60.7	65.8	64.7	58.2	-
edGNN [22]	86.9	59.8	65.7	64.4	56.3	-
GIN [25]	89.4 \pm 5.6	64.3 \pm 10.0	65.3 \pm 5.6	64.8 \pm 5.9	64.6 \pm 7.0	76.2 \pm 2.8
RW-GNN [26]	89.2 \pm 4.3	61.0 \pm 1.5	63.0 \pm 2.1	63.1 \pm 1.9	56.1 \pm 1.2	74.7 \pm 3.3
DropGNN [51]	90.4 \pm 7.0	63.2 \pm 5.1	66.3 \pm 8.6	64.8 \pm 4.5	65.1 \pm 5.2	76.3 \pm 6.1
IEGN [52]	84.6 \pm 10.0	60.8 \pm 3.0	59.8 \pm 1.4	61.1 \pm 2.1	59.5 \pm 7.3	75.2 \pm 4.3
Gra+QSVM [1]	81.80 \pm 10.3	60.66 \pm 5.4	62.50 \pm 10.2	57.50 \pm 8.8	60.89 \pm 7.3	71.10 \pm 6.6
Gra+QCNN [4]	81.04 \pm 14.1	59.86 \pm 10.9	63.2 \pm 11.2	58.96 \pm 9.9	61.53 \pm 8.6	77.05 \pm 10.1
Gra+QCNN (w/ M) [4]	81.88 \pm 9.3	61.88 \pm 3.5	64.8 \pm 4.11	61.25 \pm 5.53 1	62.02 \pm 3.3	78.9 \pm 7.8
GraphQNTK [13]	88.4 \pm 6.5	-	-	-	62.9 \pm 5.0	71.1 \pm 3.2
egoQGNN (w/o M)	82.28 \pm 10.53	60.35 \pm 6.4	64.40 \pm 9.4	60.71 \pm 2.2	62.84 \pm 8.3	70.51 \pm 5.6
egoQGNN	85.83 \pm 3.7	64.57 \pm 4.6	67.3 \pm 5.6	65.67 \pm 2.5	65.14 \pm 5.6	79.78 \pm 4.7

the datasets, the nodes have the categorical input features required for egoQGNN.

- **MUTAG:** The graphs contained in this dataset represent heteroaromatic nitro or mutagenic aromatic compounds. The nodes and edges represent atoms and chemical bonds, respectively. The nodes labels represent the chemical identity of the atoms. All of the graphs in this dataset belong to one of two classes which represent whether the graph has a mutagenic effect or not.
- **PTC:** The Predictive Toxicology Challenge (PTC) has four variants, representing molecule carcinogenicity on male mice (PTC_MM), male rats (PTC_MR), female mice (PTC_FM), female rats (PTC_FR), respectively. The graphs from each variant are labeled by their carcinogenicity on male and female mice and rats.
- **PROTEINS:** This dataset includes two classes of proteins. The first is enzymes, while the second is non-enzymes. Nodes represent the different amino acids belonging to the proteins. Edges represent whether the distance between pairs of amino acids is less than 0.6 nanometres.

To the best of our knowledge, GraphQNTK [13] is one of the few currently available (and also the most up-to-date) quantum algorithms that can be applied to realistically sized real-world graph datasets. In fact, for the typical quantum algorithms, QSVM [1] and QCNN [9], due to the limitations on the number of qubits, high-dimensional graph

data cannot be handled directly. Fortunately, Yanardag et al. [56] proposed a method based on the number of graphlets to encode high-dimensional graphs using low-dimensional representations. We, therefore, use this method to encode a high-dimensional graph as an 8-dimensional vector and then use this vector as the input to both QSVM and QCNN. Additionally, we compare egoQGNN with several state-of-the-art baselines for graph classification:

(1) The kernel based models: WL subtree kernel [49] and Subgraph Matching Kernel (CSM) [50].

(2) The state-of-the-art GNNs: These include Diffusion convolutional neural networks (DCNN) [57], Deep Graph CNN (DGCNN) [31] and Relational Graph Convolutional Networks (R-GCN) [24], Graph Isomorphism Network (GIN) [22] and edGNN [25], Random Walk Graph Neural Networks (RW-GNN) [26], Dropout Graph Neural Networks (DropGNN) [51], Invariant-Equivariant Graph Network (IEGN) [52].

5.2 Experimental Setup

For experiments, we use three Ulayers in egoQGNN. All three Ulayers have identical structures but no shared parameters. In the quantum circuit of the mapping method, the feature of a node can be mapped to several qubits. In experiments, we map the feature of each node into a qubit since the node features of the datasets are simple (a scalar). The quantum circuits of the proposed method are similar to QCNN and QSVM, and RX, RY, RZ gates are applied on each qubit sequentially. During the training, UOBYQA [58],

which is based on a derivative-free optimization method, is used to optimize the egoQGNN.

Due to the lack of qubits, QSVM only accepts 2-dimensional or 3-dimensional data. So, we use PCA to transform an 8-dimensional graphlet frequency counts vector into a 3-dimensional vector. The quantum machine learning methods are run in simulation on a classical computer. The code for QSVM is provided by Qiskit [59], and the code for QCNN is provided by Tensorflow Quantum [60].

The results for the deep learning methods mostly come from the existing studies [25] [22]. Using the available codes provided by the authors, we perform 10-fold cross-validation to compute the accuracies of GIN and DGCNN on the PTC_FM, PTC_MM and PTC_FR datasets, and both R-GCN and edGNN on the PROTEINS dataset. The parameters for the deep learning methods are those provided by the authors.

For fairness, all of the methods compared are run on the same computing device, namely an Intel Xeon CPU E3-1270 v5 with 32GB RAM. The proposed method is implemented using the OriginQ [61] simulator on a classical computer. As yet existing quantum coding platforms [59], [60] are unable to provide the fast and effective interaction between a classical computer and a quantum computer required by the proposed framework. For this reason, all of the reported experiments are performed using a simulator running on a classical computer.

5.3 Results and Discussion

The performances on graph classification are assessed in terms of accuracy. We report the average and standard deviation of the 10-fold validation accuracies. The results achieved by egoQGNN are reported in Table 4. We also give the performance achieved by egoQGNN without the trainable mapping method. This is done to demonstrate the effectiveness of the mapping strategy described in Section IV.

5.3.1 Comparison with machine learning methods

For the evaluation, we employ the same structure for the proposed egoQGNN model on all of the graph datasets studied. Results in Table 4 indicate that egoQGNN achieves the best results on 5 out of the 7 benchmarks, showing that in many cases a clear improvement is obtained with respect to the GNN models. The accuracies of the egoQGNN with a trainable mapping method on PTC_FM and PTC_MM are 64.57 ± 4.64 and 65.67 ± 2.54 respectively, which are roughly equivalent to less powerful methods. For PTC_FR and PTC_MR, egoQGNN achieves 1.96 and 0.54 improvements over the next-best performing methods. Besides, even in the cases where egoQGNN does not achieve top performance, its accuracy is close to that of the GNNs studied.

5.3.2 Comparison with alternative quantum machine learning methods

Gra+QSVM and Gra+QCNN in Tabel 4 refer to using the graphlet count vector as the input to QSVM and QCNN, respectively. QSVM has its mapping circuit shown in the Appendix but QCNN does not. We apply the mapping circuits shown in Fig. 1 to QCNN (Gra+QCNN (w/ M)).

The results of Gra+QSVM, Gra+QCNN and Gra+QCNN (w/ M) represent no improvement on egoQGNN. Moreover, compared to Gra+QCNN, Gra+QCNN (w/ M) achieves higher accuracy. Notably, compared to GraphQNTK, our model performs better on all datasets except MUTAG. The reason for this may be the hierarchical structure of our model, which is not adopted in GraphQNTK. This demonstrates that our proposed trainable mapping method is also effective when combined with alternative quantum machine learning algorithms.

5.3.3 Comparison of egoQGNN (w/o M) and egoQGNN

We observe that egoQGNN when combined with our trainable mapping method slightly and consistently outperforms egoQGNN without this trainable mapping i.e. egoQGNN (w/o M). Since they have the same structure, the improvement may be attributed to less information loss compared to the egoQGNN without the mapping method. Note that the accuracy of egoQGNN is about 9% higher than egoQGNN (w/o M) on the PROTEINS dataset, while for the MUTAG dataset, the accuracy of egoQGNN (w/o M) is close to that of egoQGNN. Table 4 shows that PROTEINS uses 61 node labels while MUTAG uses only seven. This means that the PROTEINS dataset requires higher dimensionality for the node features and suffers more serious information loss. The results show that our trainable mapping method reduces information loss and improves performance. Besides, for most datasets, the standard error for egoQGNN is less than that for egoQGNN (w/o M). For example, the standard errors for egoQGNN (w/o M) and egoQGNN on PTC_FR are respectively 9.4 and 5.6. When there is no trainable mapping, the elements of the node feature vector are used as the gate parameters to map data to quantum states. This leads to a random distribution of quantum states in the Hilbert space.

5.3.4 Comparison of parameters

Compared with the deep learning methods, egoQGNN has fewer parameters but achieves comparable performance, as shown in Table 5. One of the possible reasons is that as mentioned in [7], the Hilbert space is a high-dimensional space, and the performance of quantum machine learning algorithms can be improved even though their parameters are fewer in number. For example, for a 32-dimension input, a layer of a GNN model requires a 32×32 weight matrix to transform the input to a 32-dimension output. As a result, this layer has 1024 parameters. For quantum machine learning, the entanglement of 5 qubits generates 32-dimensional quantum states. Suppose that three quantum gates are applied to each qubit and each quantum gate has a parameter. In this instance, the quantum machine learning model transforms a 32-dimensional quantum state to a new 32-dimensional quantum state as output using only 15 parameters. Besides, similar to [38], egoQGNN captures the feature of the nodes in a non-Euclidean space. This reduces the distortion and leads to an improvement in performance.

5.3.5 Comparison of run-times

We report the average run times of egoQGNN and the baselines on MUTAG in Fig 5. For fairness, all the methods

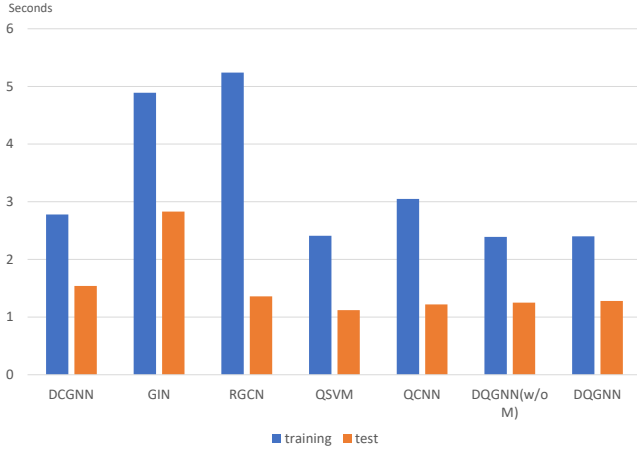


Fig. 5. Running time comparison on MUTAG. The blue and orange bars indicate the per-epoch training time and test time respectively.

TABLE 5

Quantum model parameter size (the number of parameters) comparison. The parameters of GNN include all the parameters of the weight matrix to be trained. The parameters of the quantum algorithm are the angles required by all of the quantum gates (unitary matrix).

Quantum model	Parameter size
DGCNN [31]	2,560
R-GCN [24]	16,704
edGNN [22]	9,345
GIN [25]	13,000
QSVM [1]	36
QCNN [4]	54
egoQGNN (w/o M)	36
egoQGNN	43

run on a machine with an Intel Xeon CPU E3-1270 v5. The run-time of the proposed method is comparable to the alternative quantum methods and superior to several of the deep learning methods. One important observation is that egoQGNN is less time-consuming than QCNN and close in performance to QSVM. It is worth noting that deep learning based methods, i.e. DCGNN, GIN and RGCN are no faster than the quantum computing methods since the comparison is executed on a conventional CPU-based machine.

6 CONCLUSIONS AND OUTLOOK

In this paper, we have developed a novel hybrid quantum-classical algorithm for graph-structured data, namely the Ego-graph based Quantum Graph Neural Network (ego-QGNN). We have introduced the theoretical framework of the egoQGNN and provided mathematical proof concerning its ability to identify graph isomorphisms. We also propose a decompositional processing strategy, which liberates egoQGNN from the limitation of the number of qubits. With the aid of classical computers, egoQGNN can handle graphs with larger sizes as input on a quantum device of a given size. Moreover, to reduce information loss during the mapping of data to quantum states, a trainable method is proposed. Experimental results demonstrate this method is beneficial and leads to improvements in the performance of quantum machine learning algorithms. There are several potentially interesting directions for future work. As

a long-term goal, quantum techniques need to be utilized to achieve exponential speed-up. In the short term, given the fast methodological developments [62], [63], [64] on the node-level embedding with classic computers, it is also imperative to develop competitive quantum counterparts that are feasible on near-term quantum devices. A natural extension for quantum node embedding is to develop quantum solvers for the problem of combinatorial optimization e.g. graph matching [65], [66], since there are a few quantum solvers [67] and these are yet not learnable.

ACKNOWLEDGMENT

This work was partly supported by National Key Research and Development Program of China (2020AAA0107600), National Natural Science Foundation of China (62176227, U2066213 and 62222607), the fundamental research funds for the central universities under grant 2072021004 and Shanghai Municipal Science and Technology Project (22511105100).

APPENDIX

Proof of the Lemma 1:

For four different quantum states A, B, C, D satisfying the following condition:

$$A \otimes B = C \otimes D \quad (20)$$

Suppose A, C are n -dimensional quantum states, B, D are m -dimensional quantum states. The a_i, b_j, c_i, d_j are i -th or j -th components of A, B, C, D respectively. So, the above formula can be rewritten as:

$$a_i b_j = c_i d_j \quad (i, j \in N^*, i \leq n, j \leq m) \quad (21)$$

So, for any $k \in [1, m], k \in N^*$:

$$\begin{cases} a_1 b_k = c_1 d_k \\ a_2 b_k = c_2 d_k \\ \vdots \\ a_n b_k = c_n d_k \end{cases} \quad (22)$$

Obviously, the A, C are linear correlations. Suppose $d_k/b_k = \varepsilon, \varepsilon \in \mathbb{R}$:

$$a_i/c_i = d_k/b_k = \varepsilon \quad (23)$$

$$a_i = \varepsilon \cdot c_i \quad (24)$$

$$A = \varepsilon \cdot C \quad (25)$$

Thus, the B, D are also linear correlations.

$$A \otimes B = C \otimes D \quad (26)$$

$$\varepsilon \cdot C \otimes B = C \otimes D \quad (27)$$

Eq.(22) can be rewritten as:

$$\begin{cases} \varepsilon \cdot c_1 b_k = c_1 d_k \\ \varepsilon \cdot c_2 b_k = c_2 d_k \\ \vdots \\ \varepsilon \cdot c_n b_k = c_n d_k \end{cases} \quad (28)$$

Naturally, $B = \frac{1}{\varepsilon} \cdot D$, the B, D are linear correlation. This means that the tensor product does not map non-zero

vectors to the same representation unless they are linearly correlated.

Proof of the Lemma 2:

For two linearly dependent quantum states: A and B , $B = k \cdot A$, $k \in \mathbb{R}$. Suppose A and B are n -dimensional quantum states, the a_i and b_i are the i -th components of A and B respectively. According to the property of quantum states:

$$\sum_{i=1}^n |a_i|^2 = \sum_{i=1}^n |b_i|^2 = 1 \quad (29)$$

A and B are linearly dependent quantum states and $B = k \cdot A$. Thus, the above formula can be rewritten as:

$$\sum_{i=1}^n |b_i|^2 = \sum_{i=1}^n |k \cdot a_i|^2 = k^2 \sum_{i=1}^n |a_i|^2 = \sum_{i=1}^n |a_i|^2 \quad (30)$$

So, $k = 1$ or $k = -1$. It means that if A and B are linearly dependent quantum states, $|A| = |B|$.

Proof of the Lemma 3:

For nodes v and μ , suppose $|\varphi_v\rangle^t$ and $|\varphi_\mu\rangle^t$ are quantum states of v and μ in t -th layer respectively. There are two situations for v and μ :

- (1) v and μ have different numbers of neighbors.
If v and μ have different numbers of neighbors, the dimensions of $|\varphi_v\rangle$ and $|\varphi_\mu\rangle^{t-1}$ are different. The $|\varphi_v\rangle^{t-1}$ and $|\varphi_\mu\rangle^{t-1}$ are 2-dimensional quantum states, because each node is represented by a qubit. The quantum state of a qubit is 2-dimensional. So, if v and μ have different numbers of neighbors, the dimensions of $|\varphi_v\rangle^t$ and $|\varphi_\mu\rangle^t$ are different, $|\varphi_v\rangle^t \neq |\varphi_\mu\rangle^t$.
- (2) v and μ have the same number of neighbors.
The Eq. 10 can be rewritten as below:

$$|\varphi_v\rangle^t = \sigma(U_1 |\varphi_v\rangle^{t-1} \bigotimes |\varphi_{N_v}\rangle^{t-1}) \quad (31)$$

$$|\varphi_\mu\rangle^t = \sigma(U_1 |\varphi_\mu\rangle^{t-1} \bigotimes |\varphi_{N_\mu}\rangle^{t-1}) \quad (32)$$

$$|\varphi_{N_v}\rangle^{t-1} = \bigotimes_{i \in N(v)} U_2 |\varphi_i\rangle^{t-1} \quad (33)$$

$$|\varphi_{N_\mu}\rangle^{t-1} = \bigotimes_{i \in N(\mu)} U_2 |\varphi_i\rangle^{t-1} \quad (34)$$

$$(35)$$

According to Lemma 1 and Lemma 2, the tensor product maps two quantum states, A and B , to the same representation if and only if $A = B$ or $A = -B$. Therefore, $|\varphi_v\rangle^{t-1} \neq |\varphi_\mu\rangle^{t-1}$, $|\varphi_v\rangle^t \neq |\varphi_\mu\rangle^t$.

Proof of Theorem 4:

Suppose for two non-isomorphic graphs G_1 and G_2 , the collections of representations of all nodes in the last layer of GNN are $\{h_v^K | v \in G_1\}$ and $\{h_\mu^K | \mu \in G_2\}$ respectively. Similarly, the collections of representations of all nodes in the last layer of egoQGNN are $\{|\varphi_v\rangle^K | v \in G_1\}$ and $\{|\varphi_\mu\rangle^K | \mu \in G_2\}$. If GNNs decide G_1 and G_2 are non-isomorphic, $\exists h_v^K \neq h_\mu^K$ ($v \in G_1, \mu \in G_2$). According to Lemma 1-3, for egoQGNN, $\exists |\varphi_v\rangle^K \neq |\varphi_\mu\rangle^K$ ($v \in G_1, \mu \in G_2$). Moreover, according to the Eq. 11:

$$h_{G_1} = \sum_{v \in G_1} S(\rho_v), h_{G_2} = \sum_{\mu \in G_2} S(\rho_\mu) \quad (36)$$

$$h_{G_1} \neq h_{G_2} \quad (37)$$

The representations of G_1 and G_2 are unequal to each other. So, egoQGNN can distinguish graphs that are decided as non-isomorphic by GNNs.

REFERENCES

- [1] V. Havlíček, A. D. Córcoles, K. Temme, A. W. Harrow, A. Kandala, J. M. Chow, and J. M. Gambetta, "Supervised learning with quantum-enhanced feature spaces," *Nature*, vol. 567, no. 7747, pp. 209–212, 2019.
- [2] M. Schuld and N. Killoran, "Quantum machine learning in feature Hilbert spaces," *Physical Review Letters*, 2018.
- [3] S. Lu and S. Braunstein, "Quantum decision tree classifier," *Quantum information processing*, vol. 3, no. 13, pp. 757–777, 2014.
- [4] I. Cong, S. Choi, and M. D. Lukin, "Quantum convolutional neural networks," *Nature Physics*, vol. 15, no. 12, pp. 1273–1278, 2019.
- [5] L. Hu, S.-H. Wu, W. Cai, Y. Ma, X. Mu, Y. Xu, H. Wang, Y. Song, D.-L. Deng, C.-L. Zou, and L. Sun, "Quantum generative adversarial learning in a superconducting quantum circuit," *Science Advances*, vol. 5, no. 1, 2019. [Online]. Available: <https://advances.sciencemag.org/content/5/1/eaav2761>
- [6] G. Verdon, T. McCourt, E. Lutzchnica, V. Singh, S. Leichenauer, and J. Hidary, "Quantum graph neural networks," 2019.
- [7] Maria and Schuld, "Machine learning in quantum spaces." *Nature*, 2019.
- [8] V. N. Vapnik and A. Chervonenkis, "A note on one class of perceptrons," *Automation and Remote Control*, vol. 25, jan 1964.
- [9] M. Schlichtkrull, T. N. Kipf, P. Bloem, R. van den Berg, I. Titov, and M. Welling, "Modeling relational data with graph convolutional networks," in *15th International Conference on Extended Semantic Web Conference, ESWC 2018*. Springer/Verlag, 2018, pp. 593–607.
- [10] J. Zheng, Q. Gao, and Y. Lü, "Quantum graph convolutional neural networks," in *2021 40th Chinese Control Conference (CCC)*. IEEE, 2021, pp. 6335–6340.
- [11] P. Mernyei, K. Meichanetzidis, and I. I. Ceylan, "Equivariant quantum graph circuits," in *International Conference on Machine Learning*. PMLR, 2022, pp. 15401–15420.
- [12] G. Yan, Y. Tang, and J. Yan, "Towards a native quantum paradigm for graph representation learning: A sampling-based recurrent embedding approach," in *Proceedings of the 28th ACM SIGKDD Conference on Knowledge Discovery and Data Mining, 2022*, pp. 2160–2168.
- [13] J. Y. Yehui Tang, "GraphQNTK: the quantum neural tangent kernel for graph data," in *Proceedings of the 36th International Conference on Neural Information Processing Systems, 2022*.
- [14] S. S. Du, K. Hou, R. R. Salakhutdinov, B. Póczos, R. Wang, and K. Xu, "Graph neural tangent kernel: Fusing graph neural networks with graph kernels," *Advances in neural information processing systems*, vol. 32, 2019.
- [15] T. Hamaguchi, H. Oiwa, M. Shimbo, and Y. Matsumoto, "Knowledge transfer for out-of-knowledge-base entities : A graph neural network approach," in *Proceedings of the Twenty-Sixth International Joint Conference on Artificial Intelligence, IJCAI-17, 2017*, pp. 1802–1808. [Online]. Available: <https://doi.org/10.24963/ijcai.2017/250>
- [16] W. Hamilton, Z. Ying, and J. Leskovec, "Inductive representation learning on large graphs," in *Advances in Neural Information Processing Systems 30*, I. Guyon, U. V. Luxburg, S. Bengio, H. Wallach, R. Fergus, S. Vishwanathan, and R. Garnett, Eds. Curran Associates, Inc., 2017, pp. 1024–1034. [Online]. Available: <http://papers.nips.cc/paper/6703-inductive-representation-learning-on-large-graphs.pdf>
- [17] T. N. Kipf and M. Welling, "Semi-supervised classification with graph convolutional networks," 2017.
- [18] A. Sanchez-Gonzalez, N. Heess, J. T. Springenberg, J. Merel, M. Riedmiller, R. Hadsell, and P. Battaglia, "Graph networks as learnable physics engines for inference and control," in *International Conference on Machine Learning*. PMLR, 2018, pp. 4470–4479.
- [19] P. Battaglia, R. Pascanu, M. Lai, D. J. Rezende, and K. Kavukcuoglu, "Interaction networks for learning about objects, relations and physics," in *Proceedings of the 30th International Conference on Neural Information Processing Systems, 2016*, pp. 4509–4517.
- [20] E. B. Khalil, H. Dai, Y. Zhang, B. Dilkina, and L. Song, "Learning combinatorial optimization algorithms over graphs," in *NIPS*, 2017.
- [21] F. Scarselli, M. Gori, A. C. Tsoi, M. Hagenbuchner, and G. Monfardini, "The Graph Neural Network Model," *IEEE Transactions on Neural Networks*, vol. 20, no. 1, p. 61, 2009.
- [22] K. Xu, W. Hu, J. Leskovec, and S. Jegelka, "How powerful are graph neural networks?" in *International Conference on Learning Representations*, 2018.

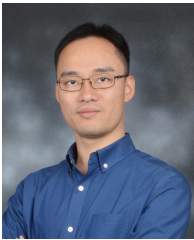
- [23] B. Weisfeiler and A. Leman, "A reduction of a Graph to a Canonical Form and an Algebra Arising during this Reduction (in Russian)," *Nauchno-Tekhnicheskaya Informatsia*, vol. 9, jan 1968.
- [24] M. Schlichtkrull, T. N. Kipf, P. Bloem, R. Van Den Berg, I. Titov, and M. Welling, "Modeling relational data with graph convolutional networks," in *European semantic web conference*. Springer, 2018, pp. 593–607.
- [25] G. Jaume, A. phi Nguyen, M. R. Martínez, J.-P. Thiran, and M. Gabrani, "edggn: a simple and powerful gnn for directed labeled graphs," 2019.
- [26] G. Nikolentzos and M. Vazirgiannis, "Random walk graph neural networks," *Advances in Neural Information Processing Systems*, vol. 33, pp. 16 211–16 222, 2020.
- [27] Y. Yang, Z. Feng, M. Song, and X. Wang, "Factorizable graph convolutional networks," *Advances in Neural Information Processing Systems*, vol. 33, 2020.
- [28] D. Sandfelder, P. Vijayan, and W. L. Hamilton, "Ego-gnns: Exploiting ego structures in graph neural networks," in *ICASSP 2021-2021 IEEE International Conference on Acoustics, Speech and Signal Processing (ICASSP)*. IEEE, 2021, pp. 8523–8527.
- [29] J. Zhao, C. Li, Q. Wen, Y. Wang, Y. Liu, H. Sun, X. Xie, and Y. Ye, "Gophormer: Ego-graph transformer for node classification," 2021.
- [30] Q. Zhu, C. Yang, Y. Xu, H. Wang, C. Zhang, and J. Han, "Transfer learning of graph neural networks with ego-graph information maximization," *Advances in Neural Information Processing Systems*, vol. 34, pp. 1766–1779, 2021.
- [31] M. Zhang, Z. Cui, M. Neumann, and Y. Chen, "An end-to-end deep learning architecture for graph classification," in *Proceedings of the AAAI Conference on Artificial Intelligence*, vol. 32, 2018.
- [32] F. Scarselli, M. Gori, A. C. Tsoi, M. Hagenbuchner, and G. Monfardini, "The graph neural network model," *IEEE transactions on neural networks*, vol. 20, no. 1, pp. 61–80, 2008.
- [33] J. Bruna, W. Zaremba, A. Szlam, and Y. Lecun, "Spectral networks and locally connected networks on graphs," in *International Conference on Learning Representations (ICLR2014)*, CBLS, April 2014, 2014, pp. http–openreview.
- [34] M. Defferrard, X. Bresson, and P. Vandergheynst, "Convolutional neural networks on graphs with fast localized spectral filtering," in *Proceedings of the 30th International Conference on Neural Information Processing Systems*, 2016, pp. 3844–3852.
- [35] O. Rippel, J. Snoek, and R. P. Adams, "Spectral representations for convolutional neural networks," in *Proceedings of the 28th International Conference on Neural Information Processing Systems-Volume 2*, 2015, pp. 2449–2457.
- [36] C. Gallicchio and A. Micheli, "Fast and deep graph neural networks," in *Proceedings of the AAAI Conference on Artificial Intelligence*, vol. 34, 2020, pp. 3898–3905.
- [37] I. Balazevic, C. Allen, and T. Hospedales, "Multi-relational poincaré graph embeddings," in *Advances in Neural Information Processing Systems*, H. Wallach, H. Larochelle, A. Beygelzimer, F. d'Alché-Buc, E. Fox, and R. Garnett, Eds., vol. 32. Curran Associates, Inc., 2019, pp. 4463–4473.
- [38] I. Chami, Z. Ying, C. Ré, and J. Leskovec, "Hyperbolic graph convolutional neural networks," in *Advances in neural information processing systems*, 2019, pp. 4868–4879.
- [39] G. Bachmann, G. Bécigneul, and O. Ganea, "Constant curvature graph convolutional networks," in *International Conference on Machine Learning*. PMLR, 2020, pp. 486–496.
- [40] Q. Liu, M. Nickel, and D. Kiela, "Hyperbolic graph neural networks," in *Advances in Neural Information Processing Systems*, 2019, pp. 8230–8241.
- [41] S. Dernbach, A. Mohseni-Kabir, S. Pal, and D. Towsley, "Quantum walk neural networks for graph-structured data," in *International Conference on Complex Networks and their Applications*. Springer, 2018, pp. 182–193.
- [42] Z. Zhang, D. Chen, J. Wang, L. Bai, and E. R. Hancock, "Quantum-based subgraph convolutional neural networks," *Pattern Recognition*, vol. 88, pp. 38–49, 2019.
- [43] C. Tüysüz, C. Rieger, K. Novotny, B. Demirköz, D. Dobos, K. Potamianos, S. Vallecorsa, J.-R. Vlimant, and R. Forster, "Hybrid quantum classical graph neural networks for particle track reconstruction," *Quantum Machine Intelligence*, vol. 3, no. 2, pp. 1–20, 2021.
- [44] S. Y.-C. Chen, T.-C. Wei, C. Zhang, H. Yu, and S. Yoo, "Hybrid quantum-classical graph convolutional network," *arXiv preprint arXiv:2101.06189*, 2021.
- [45] R. Raussendorf, "Key ideas in quantum error correction," *Philosophical Transactions of the Royal Society A: Mathematical, Physical and Engineering Sciences*, vol. 370, no. 1975, pp. 4541–4565, 2012.
- [46] P. Rebentrost, M. Mohseni, and S. Lloyd, "Quantum support vector machine for big data classification," *Physical Review Letters*, vol. 113, no. 13, p. 130503, 2014.
- [47] S. Lloyd and C. Weedbrook, "Quantum generative adversarial learning," *Physical Review Letters*, vol. 121, no. 4, pp. 040 502.1–040 502.5, 2018.
- [48] H. Situ, Z. He, Y. Wang, L. Li, and S. Zheng, "Quantum generative adversarial network for generating discrete distribution," *Information Sciences*, vol. 538, pp. 193–208, 2020.
- [49] N. Shervashidze, P. Schweitzer, E. Jan, V. Leeuwen, and K. M. Borgwardt, "Weisfeiler-lehman graph kernels," *Journal of Machine Learning Research*, vol. 1, pp. 1–48, 2010.
- [50] N. Kriege and P. Mutzel, "Subgraph matching kernels for attributed graphs," *Proceedings of the 29th International Conference on Machine Learning, ICML 2012*, vol. 2, 06 2012.
- [51] P. A. Papp, K. Martinkus, L. Faber, and R. Wattenhofer, "Dropgnn: random dropouts increase the expressiveness of graph neural networks," *Advances in Neural Information Processing Systems*, vol. 34, pp. 21 997–22 009, 2021.
- [52] H. Maron, H. Ben-Hamu, N. Shamir, and Y. Lipman, "Invariant and equivariant graph networks," in *International Conference on Learning Representations 2019*, 2019, pp. 193–196.
- [53] A. K. Debnath, R. L. L. D. Compadre, G. Debnath, A. J. Shusterman, and C. Hansch, "Structure-activity relationship of mutagenic aromatic and heteroaromatic nitro compounds. correlation with molecular orbital energies and hydrophobicity," *Journal of Medicinal Chemistry*, vol. 34, no. 2, pp. 786–797, 1991.
- [54] C. Helma, R. D. King, S. Kramer, and A. Srinivasan, "The predictive toxicology challenge 2000-2001," *Bioinformatics*, vol. 17, no. 1, pp. 107–108, 2001.
- [55] R. Lab, "Protein function prediction via graph kernels," *Oral Radiology*, vol. 6, no. 2, pp. 29–35, 1990.
- [56] P. Yanardag and S. Vishwanathan, "Deep graph kernels," in *Proceedings of the 21th ACM SIGKDD international conference on knowledge discovery and data mining*, 2015, pp. 1365–1374.
- [57] J. Atwood and D. Towsley, "Diffusion-convolutional neural networks," *Computer ence*, 2015.
- [58] M. J. D. Powell, "Uobyqa: unconstrained optimization by quadratic approximation," *Mathematical Programming*, vol. 92, no. 3, pp. 555–582, 2002.
- [59] M. Bozzo-Rey and R. Loredó, "Introduction to the ibm q experience and quantum computing," in *Proceedings of the 28th Annual International Conference on Computer Science and Software Engineering*, 2018, pp. 410–412.
- [60] M. Broughton, G. Verdon, T. McCourt, A. J. Martinez, J. H. Yoo, S. V. Isakov, P. Massey, R. Halavati, M. Y. Niu, A. Zlokapa, E. Peters, O. Lockwood, A. Skolik, S. Jerbi, V. Dunjko, M. Leib, M. Streif, D. V. Dollen, H. Chen, S. Cao, R. Wiersema, H.-Y. Huang, J. R. McClean, R. Babbush, S. Boixo, D. Bacon, A. K. Ho, H. Neven, and M. Mohseni, "Tensorflow quantum: A software framework for quantum machine learning," 2021.
- [61] xiaoyaolanyun, "Quantum computing framework: Qpanda," 2000. [Online]. Available: <https://github.com/OriginQ/QPanda-2>
- [62] T. Zhang, Q. Wu, and J. Yan, "Learning high-order graph convolutional networks via adaptive layerwise aggregation combination," *IEEE Transactions on Neural Networks and Learning Systems*, 2021.
- [63] —, "Scalecgn: Efficient and effective graph convolution via channel-wise scale transformation," *IEEE Transactions on Neural Networks and Learning Systems*, 2022.
- [64] Q. Wu, H. Zhang, J. Yan, and D. Wipf, "Handling distribution shifts on graphs: An invariance perspective," in *International Conference on Learning Representation*, 2022.
- [65] R. Wang, J. Yan, and X. Yang, "Combinatorial learning of robust deep graph matching: an embedding based approach," *IEEE Transactions on Pattern Analysis and Machine Intelligence*, 2021.
- [66] —, "Neural graph matching network: Learning lawler's quadratic assignment problem with extension to hypergraph and multiple-graph matching," *IEEE Transactions on Pattern Analysis and Machine Intelligence*, 2022.
- [67] T. Birdal, V. Golyanik, C. Theobalt, and L. Guibas, "Quantum permutation synchronization," 2021.



Xing Ai is now a PhD student at the Computing Department of Hong Kong Polytechnic University. He obtained his bachelor's degree from the Software Department of Xiamen University, China in 2015. He then received his master's degree from the Information Department of Xiamen University, China in 2019. His research interests include machine learning, graph representation, and quantum computing. He completed this paper during his study for his master's degree at Xiamen University.



Luzhe Sun is now a postgraduate student in the Department of Computer Science at the University of Chicago. His research interests include Graph Theory, Transform Learning, Quantum Computing. His recent work has focused on directed acyclic graph learning and secure trajectory planning and shared autonomy using causal inference. He completed this paper during his study for his bachelor's degree at Xiamen University.



Junchi Yan (S'10-M'11-SM'21) is currently an Associate Professor with Department of Computer Science and Engineering, Shanghai Jiao Tong University, Shanghai, China. Before that, he was a Senior Research Staff Member and Principal Scientist with IBM Research where he started his career since April 2011. He obtained the Ph.D. at the Department of Electronic Engineering of Shanghai Jiao Tong University. His research interests are machine learning, as well as the intersection with combinatorial optimization and quantum computing. He has also recently published quantum graph learning works in SIGKDD and NeurIPS. He serves as Area Chair for NeurIPS/ICML/AAAI/CVPR, etc. and Associate Editor for Pattern Recognition.



Zhihong Zhang received his BSc degree (1st class Hons.) in computer science from the University of Ulster, UK, in 2009 and the PhD degree in computer science from the University of York, UK, in 2013. He won the K. M. Stott prize for best thesis from the University of York in 2013. He is now an associate professor at the School of Informatics Xiamen University, China. His research interests are wide-reaching but mainly involve the areas of pattern recognition and machine learning, particularly problems involving graphs and networks. He is a recipient of the Best Paper Awards of the International Conference on Pattern Recognition ICPR 2018. He is currently an Associate Editor of Pattern Recognition Journal.



Edwin R. Hancock holds a B.Sc. degree in physics (1977), a Ph.D. degree in high-energy physics (1981) and a D.Sc. degree (2008) from the University of Durham, and a doctorate Honoris Causa from the University of Alicante in 2015. He is an Emeritus Professor in the Department of Computer Science at the University of York, Adjunct Professor at Beihang University and Distinguished Visiting Professor at Xiamen University. His main research interests are in pattern recognition, machine learning and computer vision, where he has made sustained contributions to the use of graph-based methods and physics-based vision over the past 30 years. He was elected a Fellow of the Royal Academy of Engineering (the UK's national academy of engineering), in 2021. He is also a Fellow of both the International Association for Pattern Recognition and the IEEE. He was the 2016 Distinguished Fellow of the BMVA. He is currently Editor-in-Chief of the journal Pattern Recognition and was founding Editor-in-Chief of IET Computer Vision from 2006 until 2012. He has also been a member of the editorial boards of the journals IEEE Transactions on Pattern Analysis and Machine Intelligence, Pattern Recognition, Computer Vision and Image Understanding, Image and Vision Computing, and the International Journal of Complex Networks. He was Vice President of the IAPR from 2016 to 2018. He has been the recipient of the Pattern Recognition Medal (1992), the IAPR Piero Zamperoni Award (2006), a Royal Society Wolfson Research Merit Award (2008), and the IAPR Pierre Devijver Award (2018). He is an IEEE Computer Society Distinguished Visitor for the period 2021-2023.